Mixed-Effects Modeling of the Plasma Kinetics of the Anti-CD8 PET Tracer [^{18}F]-2C8v144 and the Non-Binding Control Tracer [^{18}F]-2C8V145 Enables Estimates of the Total Amount of CD8 in the Body, the Fraction Present in Blood, and the Equilibrium Dissociation Constant (K_D) of [^{18}] F-2C8v144, and Predictions of Total Body Receptor Occupancy by [^{18}18F]-2C8v144

Ruediger E. Port[1,5], C. Andrew Boswell[1], Annie Ogasawara[2], Herman Gill[2], Jan Marik[2], Alice F. Tarantal[3], Eric Berg[4], Simon P. Williams[2], Gregory Z.Ferl[1]

[1]Genentech, Inc., South San Francisco, California, USA, Department of Preclinical and Translational PKPD; [2]Genentech, Inc., South San Francisco, California, USA, Department of Translational Imaging; [3]Department of Pediatrics and Department of Cell Biology and Human Anatomy, School of Medicine, and California National Primate Research Center, University of California Davis, Davis, California; [4]Department of Biomedical Engineering, University of California Davis, Davis, California; [5]Consultant, Saarbruecken, Germany (ruediger.port@gmail.com)

1. Introduction

The success of checkpoint-inhibition immunotherapy in cancer patients hinges on the presence of CD8+ ("cytotoxic") T cells in tumors, and a variety of radiolabeled anti-CD8 PET tracers are currently being developed for evaluating individual chances of success by non-invasively detecting binding to CD8 in tumors[1-5]. The radioactivity detected in tumors, however, represents bound and unbound tracer so that it can reflect binding to CD8 as well as mere distribution of unbound tracer, even in the absence of CD8. The distinction of target binding and non-specific distribution of PET tracers in tissues has successfully been achieved in the development of CNS drugs, typically by comparing tracer kinetics between a brain region containing the target receptors and a "reference" region devoid of the receptors, with presumably the same parameters of non-specific tracer distribution[6,7]. No such reference tissue exists for individual malignant tumors. Instead, we are developing a non-binding control tracer, [^{18}F]-2C8v145 ("C"), which is structurally almost identical to our anti-CD8 tracer [^{18}F]-2C8v144 (binding tracer, "B"), in order to monitor first C, second B in blood and tumor, and compare the kinetics of C and B in tumor by assuming the same parameters of non-specific distribution and systemic elimination for both tracers[8-10].

The purpose of our PK study in non-human primates was 1) to assess exposure to radioactivity of C and B from PET sessions, and 2) to derive the plasma concentration-time course of C and of unbound B, i.e. the vascular input functions for analyzing the kinetics in malignant tumors.

2. Theoretical

The PK model for C was a linear three-compartment model (Fig. 2, black boxes) while the PK model for B was a variant of the classical TMDD model[11] with completely reversible target binding within and outside of circulating blood (Fig. 2, black + red boxes). The parameters of non-specific distribution and elimination were assumed to be the same for C and B. The model also assumes that: 1) there is no non-specific uptake of C or B into cells during the one-hour measuring period, 2) binding of B is completely reversible (no internalization of receptor-ligand complex [8,9]); 3) all target receptors on circulating CD8+ cells are available to B in plasma for binding:

$$\frac{dCu_1(t)}{dt} = \Big[I(t) - (CL + CL_{121} + CL_{131}) \cdot (Cu_1(t) + Cl_{121} \cdot Cu_2(t) + CL_{131} \cdot Cu_3(t) - k_{on.4} \cdot (R_4 - A_4(t) \cdot Cu_1(t) - k_{on.p} \cdot (R_b - A_{p.b}(t) \cdot Cu_1(t) + k_4 \cdot A_4(t) + k_{off.b} \cdot A_{p.b}\Big] / V_1 \quad (1)$$

$$\frac{dCu_2(t)}{dt} = CL_{121} \cdot (Cu_1(t) - Cu_2(t))/V_2 \quad (2)$$

$$\frac{dCu_3(t)}{dt} = CL_{131} \cdot (Cu_1(t) - Cu_3(t))/V_3 \quad (3)$$

$$\frac{dA_4(t)}{dt} = k_{on.4} \cdot (R_4 - A_4(t) \cdot Cu_1(t) - k_{off.4} \cdot A_4(t) \quad (4)$$

$$\frac{dA_{p.b}(t)}{dt} = k_{on.b} \cdot (R_b - A_{p.b}(t) \cdot Cu_1(t) - k_{off.b} \cdot A_{p.b}(t) \quad (5)$$

where Cu_1, Cu_2, Cu_3 are *unbound* tracer concentrations in compartments 1-3 with volumes V_1, V_2, V_3; $I(t)$ is the rate of tracer input; CL is elimination clearance, CL_{121}, CL_{131} are distribution clearances ($CL_{121} > CL_{131}$), and $A_4(t)$, $A_{p.b}(t)$, R_4, R_b are the molar amounts of bound B and of the target receptors, respectively, outside the circulation and in blood plasma. $k_{on.p}$ was assumed to be equal to k_{on} determined *in vitro* by SPR (0.50/(nM·min)[9]), and was fixed. $k_{on.4}$, $k_{on.b} = 0$ for tracer C. Initial condition = 0 for all compartments.

Individual volume and clearance parameters, and individual amounts of target receptors were assumed to vary in proportion to individual body weight^{Pwr} where Pwr = 1 for V_1, V_1, V_3, R_4, R_b and Pwr = 0.75 for CL, CL_{121}, CL_{131}[12,13]. The equilibrium dissociation constant of B (K_D) was assumed to be the same throughout the body so that $k_{off.4} = K_D \cdot k_{on.4}$, $k_{off.b} = K_D \cdot k_{on.b}$. The parameters fitted for target binding of B were: the total amount of CD8 in the body ($R_{tb} = R_4 + R_b$), the fraction present in blood ($fR_b = R_b/R_{tb}$), $k_{on.4}$, and K_D.

Measurement model: Tracer concentration in plasma ($C_{plasma}(t)$) represents the sum of the unbound concentration in the central compartment and, in the case of B, the bound concentration in plasma:

$$C_{plasma}(t) = Cu_1(t) + A_{p.b}(t)/V_{plasma} \quad (6)$$

where $A_{p.b}(t)$ is the bound amount of B in plasma (same as in whole blood) and $A_{p.b}(t) = 0$ for C. V_{plasma} was calculated by multiplying the reported normal blood volume in monkeys, 0.0734 L/kg [14], by (individual body weight x (1 - hematocrit)).

3. Methods

Each of three rhesus monkeys underwent [^{18}F]-PET two times to monitor first C and, three days later, B in arterial blood. Individual mass doses of both tracers varied 5-fold. C and B are hydrophilic VHH peptides with MW = 14 kDa. B binds monovalently to CD8$_\alpha$ without cellular internalization of receptor-ligand complex[8,9]. The in-vitro equilibrium dissociation constant (K_D) of B with CD8 is 0.13 nM, as determined by SPR[9]). Both VHH tracer molecules were radiolabeled with Al[^{18}]F using RESCA as chelator[15], as described elsewhere[9]. Dynamic scans were obtained on the primate mini-EXPLORER [16] for 60 min at a single bed position.

NONMEM, version 7.50[17] was used for model fitting. Graphical and statistical analyses were done in R[18].

4. Results

The model for C fitted the data nearly perfectly (Fig. 3a). The estimated mean residence time (with body weight = 2 kg) was 26 min. The estimated specific binding parameters of B were as follows:

R_{tb}	1.7	nmol/kg
fR_b	0.027	
$k_{on.4}$	0.00975	1/(nM·min)
$k_{on.b}$	0.50	1/(nM·min) (fixed)
K_D	0.23	nM

The mixed-effects predictions of the data of B were almost as perfect as those for C (Fig. 3b) (facilitated by estimated inter-individual random coefficients of variation of 22%, 92%, 42% for R_{tb}, fRb, $k_{on.4}$, respectively[10]). Total body receptor occupancy by B ($RO_{tb}(t) = (A_4(t) + A_{p.b}(t)/R_{tb})$, predicted for a 20 second i.v. infusion of 16, 4, 1 nmol, at body weight = 2 kg, was still higher than 90%, 70%, 20% at one hour after the beginning of the infusion[10].

5. Discussion

Dividing the estimates of mean R_{tb} and fRb by reported numbers of CD8/cell yields estimates of CD8+ cell *numbers* which can be related to reported CD8+ cell numbers in humans suggesting only minor differences between rhesus monkeys and humans[10]. The fact that the estimate of K_D of B *in vivo*, 0.23 nM, is similar to the SPR estimate of 0.13 nM while the estimated $k_{on.4}$, 0.00975/(nM·min), is more than 50 times lower than $k_{on.b}$ (0.50/(nM·min) implies that the apparent delay of association outside the circulation, as manifested by its impact on the plasma kinetics of B, is paralleled by a similar apparent delay of dissociaton, suggesting the same rate-limiting step outside of the circulation in the forward and backward directions.

The difference between the PK profiles of B and C (Fig. 1) is in part due to higher mass doses of C in all animals. Fig. 4 shows the plasma concentrations of C scaled down in proportion to dose(B)/dose(C) to reveal the "net divergence" of B versus time from C due to the reversible target binding of B outside of and within the circulation. The divergence vanishes with increasing dose of B (Fig. 4, left to right) suggesting gradual saturation of the target receptors so that total radioactivity detected by PET is increasingly dominated by unbound B. The same phenomenon must be expected when the radioactivity-time course of B and C is monitored in malignant tumors and the target receptors of B are temporarily saturated by excessive concentrations of unbound B. Thus, it will be necessary to analyze tracer *kinetics* in tumors to extract the time course of *bound* B and derive the desired information on local CD8 density by comparison with the time course of C.

6. Conclusion

Critical preclinical information as well as interesting parameter estimates regarding total body CD8+ T cell physiology could be obtained by this pilot study in just three non-human primates, thanks to 1) the novel control/binding tracer study design, 2) extremely precise PET measurements of arterial blood tracer concentrations, and 3) mixed-effects modeling with a parsimonious semi-physiological structural model.

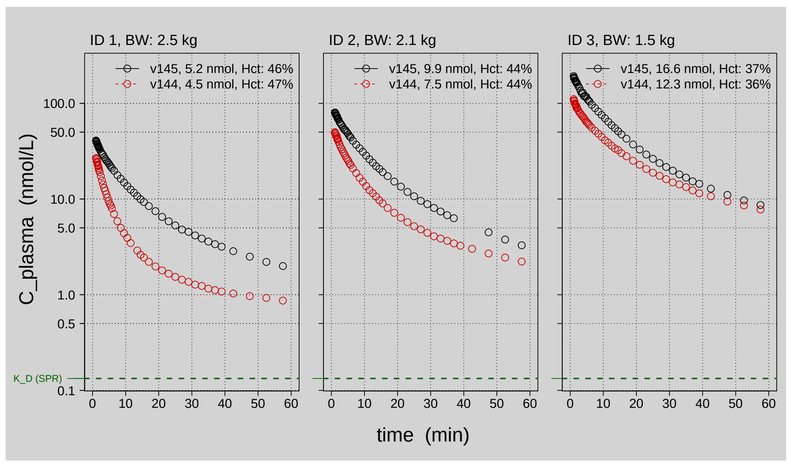

Figure 1: *Arterial plasma concentrations of* C *(black circles) and* B *(red circles) versus time after the beginning of i.v. injection. y-scale logarithmic.*

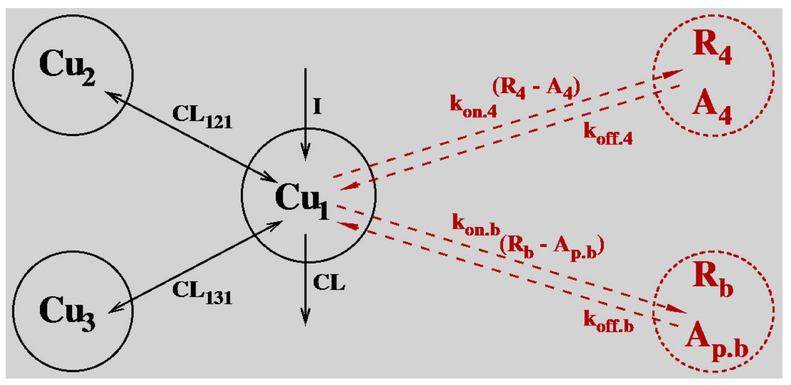

Figure 2: *Linear three-compartment model for* C *(black circles), and non-linear five-compartment model for unbound and bound* B *(black + red circles) (explanation of symbols: section 2).*

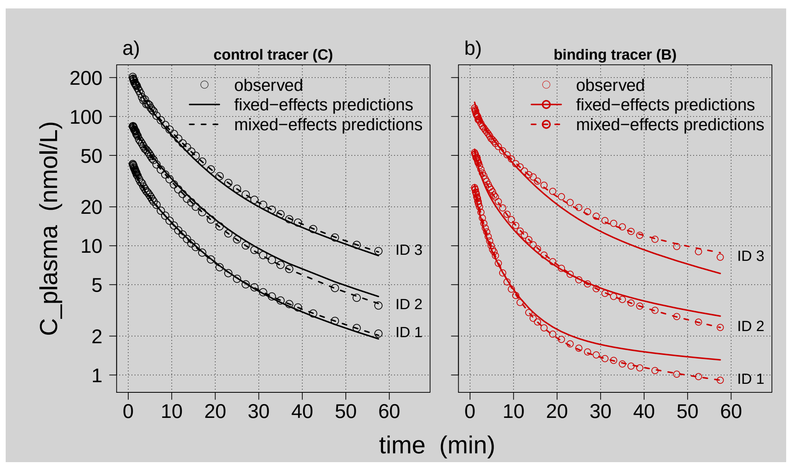

Figure 3: *Observed and predicted plasma concentrations versus time. Each set of points and curves represents one PET session in one animal. y-scale logarithmic. (Residual errors: 1.1% for* C*, 2.4% for* B*!)*

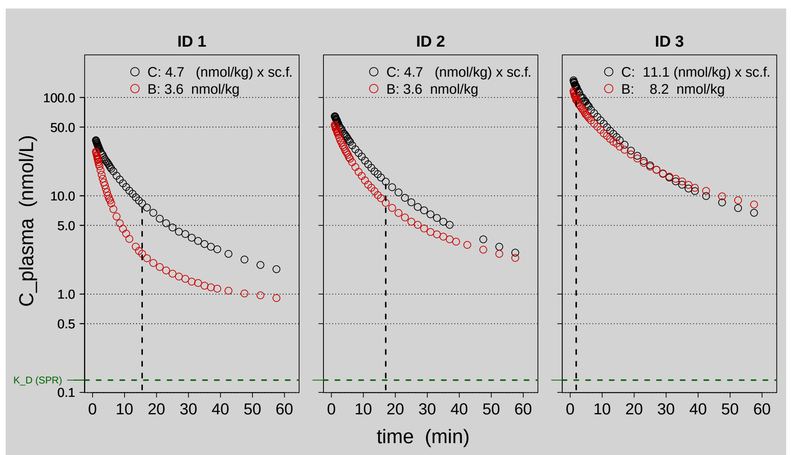

Figure 4: *Arterial plasma concentrations of* C *(black circles) and* B *(red circles) versus time after the beginning of i.v. injection where the concentrations of* C *have been multiplied by the scaling factor* `sc.f.` *= dose(*B*)/dose(*C*). y-scale logarithmic.*

7. References

[1] Farwell MD et al. J Nucl Med (2022) 63, 720-726. [2] de Ruijter KL et al. Nat Med (2022) 28, 2601-2610. [3] Tavaré R et al. Cancer Immunol Res (2022) 10, 1190-1209. [4] Wang Y et al. Eur J Nucl Med Mol Imaging (2022) 49, 4394-4405. [5] De Groof TWM et al. Eur J Nucl Med Mol Imaging (2024) 52, 193-207. [6] Innis R et al. J Cereb Blood Flow Metab (2007) 27, 1533-1539. [7] Varnaes K et al. J Pharmacokin Pharmacodyn (2013) 40, 267-279. [8] Sriraman S et al. Eur J Nucl Med Mol Imaging (2023) 50, 679-691. [9] Sriraman S et al. manuscript in preparation. [10] Port et al. J Pharmacokinet Pharmacodyn (2026) 53(3):23. doi: 10.1007/s10928-026-10029-8 . [11] Mager DE, Jusko WJ Pharmacokinet Pharmacodyn (2001) 28, 507-532. [12] Anderson BJ et al. Clin Pharmacokinet (1997) 33, 313-327. [13] West GB et al. Science (1997) 276, 122-126. [14] Davies B, Morris T, Pharm Res (1993) 10, 1093–1095. [15] Cleeren F et al., Theranostics (2017) 7, 2924-2939. [16] Berg E et al. J Nucl Med (2020) 61, 453-460. [18] https://nonmem.iconplc.com/nonmem750. [18] https://www.R-project.org.